PORTLAND PRESS

Clinical Science

ACCEPTED MANUSCRIPT

Polydatin post-treatment alleviates myocardial ischemia/reperfusion injury by promoting autophagic flux

Yuanna Ling, Guiming Chen, Yi Deng , Huixiong Tang , Long Ling, Xiaoming Zhou, Xudong Song , Pingzhen Yang , Yingfeng Liu , Zhiliang Li , Cong Zhao, Yufei Yang , Xianbao Wang, Masafumi Kitakaze , Yulin Liao, Aihua Chen

Polydatin (PD), a resveratrol glycoside, has a stronger anti-oxidative effect than resveratrol. It is known that resveratrol is an autophagic enhancer and exerts a cardioprotective effect against ischemia/reperfusion (I/R) injury. However, the effect of PD post-treatment on myocardial I/R injury remains unclear. In this study, we investigated the influences of PD post-treatment on myocardial I/R injury and autophagy. C57BL/6 mice underwent left coronary artery occlusion and cultured neonatal rat cardiomyocytes (NRCs) subjected to hypoxia were treated with vehicle or PD during reperfusion or re-oxygenation. We noted that PD enhanced autophagy and decreased apoptosis during I/R or hypoxia/reoxygenation (H/R), and this effect was antagonized by co-treatment with adenovirus carrying short hairpin RNA for Beclin 1 and 3-methyladenine (3-MA)， an autophagic inhibitor. Compared with vehicle-treated mice, PD-treated mice had a significantly smaller myocardial infarct size and a higher left ventricular fractional shortening and ejection fraction, while these effects were partly reversed by 3-MA. Furthermore, in the PD-treated NRCs, tandem fluorescent mRFP-GFP-LC3 assay showed abundant clearance of autophagosomes with an enhanced autophagic flux. And co-treatment with

Cite as Clinical Science (2016) DOI: 10.1042/CS20160082

Polydatin post-treatment alleviates myocardial ischemia/reperfusion injury by promoting autophagic flux

Yuanna Ling[1]*, Guiming Chen[3]*, Yi Deng[1], Huixiong Tang[1], Long Ling[4], Xiaoming Zhou[5], Xudong Song[1], Pingzhen Yang[1], Yingfeng Liu[1], Zhiliang Li[1], Cong Zhao[1], Yufei Yang[1], Xianbao Wang[1#], Masafumi Kitakaze[1], Yulin Liao[1,2], Aihua Chen[1#]

[1] Sino-Japan Collaborative Laboratory for Heart Failure Translating Medicine, Department of Cardiology, Zhujiang Hospital of Southern Medical University, No.253, Middle Gongye Avenue, 510282, Guangzhou, China
[2]State Key Laboratory of Organ Failure Research, Department of Cardiology, Nanfang Hospital, Southern Medical University, 510515, Guangzhou, China
[3] Department of Pathophysiology, Southern Medical University, No.1838, Northern Guangzhou Avenue, 510515, Guangzhou, China
[4] Department of Cardiology, 421 Hospital of Chinese People's Liberation Army, No.468, Xingang Road, 510318, Guangzhou, China
[5] Department of Rehabilitation, the Sixth Affiliated Hospital of Sun Yat-Sen University, No.26, Yuanchun Er Henglu, 510655, Guangzhou, China
* These authors contributed equally to this article.
# Corresponding author

Key words: polydatin; ischemia/reperfusion; autophagy; apoptosis; mitochondrial function.

Short title: Cardioprotection by polydatin post-treatment

Correspondence: Prof. Aihua Chen (email zj_chenaihua@126.com) or Dr. Xianbao Wang (email wxb2007wxb@126.com)

Abbreviations: RES, resveratrol; PD, polydatin; ROS, reactive oxygen species; AMI, acute myocardial infarction; I/R, ischemia/reperfusion; H/R, hypoxia/reoxygenation; NRCs, neonatal rat cardiomyocytes; LVFS, left ventricular fractional shortening; EF, ejection fraction.

ABSTRACT

Polydatin (PD), a resveratrol glycoside, has a stronger anti-oxidative effect than resveratrol. It is known that resveratrol is an autophagic enhancer and exerts a cardioprotective effect against ischemia/reperfusion (I/R) injury. However, the effect of PD post-treatment on myocardial I/R injury remains unclear. In this study, we investigated the influences of PD post-treatment on myocardial I/R injury and autophagy. C57BL/6 mice underwent left coronary artery occlusion and cultured neonatal rat cardiomyocytes (NRCs) subjected to hypoxia were treated with vehicle or PD during reperfusion or re-oxygenation. We noted that PD enhanced autophagy and decreased apoptosis during I/R or hypoxia/reoxygenation (H/R), and this effect was antagonized by co-treatment with adenovirus carrying short hairpin RNA for Beclin 1 and 3-methyladenine (3-MA)，an autophagic inhibitor. Compared with vehicle-treated mice, PD-treated mice had a significantly smaller myocardial infarct size and a higher left ventricular fractional shortening and ejection fraction, while these effects were partly reversed by 3-MA. Furthermore, in the PD-treated NRCs, tandem fluorescent mRFP-GFP-LC3 assay showed abundant clearance of autophagosomes with an enhanced autophagic flux. And co-treatment with Bafilomycin A1, a lysosomal inhibitor, indicated that PD promoted the degradation of autolysosome. In addition, PD post-treatment reduced mitochondrial membrane potential and cellular ROS production in NRCs, and these effects were partially blocked by Bafilomycin A1. These findings indicate that PD post-treatment limits myocardial I/R injury by promoting autophagic flux to clear damaged mitochondria to reduce ROS and cell death.

INTRODUCTION

Acute myocardial infarction (AMI) is one of the main causes of morbidity and mortality in coronary heart disease. Timely reperfusion is required to prevent cardiomyocyte loss and limit infarct size, but the accompanying ischemia/reperfusion (I/R) injury is associated with poor prognoses and causes mitochondrial oxidative stress and cell death [1, 2]. Both ischemic pre- and post-conditioning can confer cardioprotection against I/R injury [3]. While post-conditioning is a more attractive approach which is possible for clinical manipulation. And pharmacological intervention at the onset of reperfusion is feasible to mimic ischemic post-conditioning.

Polydatin (PD) and resveratrol (RES) are both natural monocrystalline compounds extracted from *Polygonum Cuspidatum*. The difference between PD (3,4,5-trihydroxystilbene-3-β-mon-D-glucoside) and RES (3,4,5-trihydroxystilbene) is the substitution of a glucoside group at the position C-3 of PD instead of a hydroxyl group [4] (Fig. 1A). Similar to RES, PD exerts multiple pharmacological effects, such as anti-oxidant and anti-inflammatory activity [4, 5], and alleviation of pressure overload-induced cardiac remodeling [6, 7]. Further, PD has more potent anti-oxidant effects than RES due to its specialized biological properties resulting from the conformational difference from RES [4, 8]. Previous studies indicate that RES and PD have cardioprotective effects if administrated before ischemia [9, 10], however it remains unclear whether PD post-treatment can potentially protect against myocardial I/R injury.

Autophagy is a controlled lysosomal-dependent catabolic process, which is involved in the degradation of long-lived proteins, as well as removing excess or damaged organelles such as mitochondria [11]. Previous studies indicate that RES pre-treatment increased cardiomyocyte survival via autophagic induction [12], while the role of PD post-treatment on autophagy during myocardial I/R is unknown. Considering the close association between oxidative stress and autophagy [13] and the powerful anti-oxidative property of PD, we hypothesized that PD treatment during reperfusion would attenuate I/R injury by enhancing autophagy.

This study aimed to assess the effects of PD post-treatment on myocardial I/R injury and to clarify its underlying mechanisms involving autophagy.

MATERIALS AND METHODS

I/R mouse model

All experiments were performed in accordance with the Guidelines for the Care and Use of Laboratory Animals (National Institutes of Health publication, No. 86-23, revised 1996) and were approved by the Bioethics Committee of the Southern Medical University. All animals used received ethical and humane care and were housed under standard conditions with a light/dark cycle of 12 h and free access to food and water. Adult male wild-type C57BL/6 mice (6–8 weeks; 20–25 g) were provided by the Laboratory Animal Center of Guangdong Province. Mice were anesthetized with a mixture of 5 mg/kg xylazine and 100 mg/kg ketamine by intraperitoneal injection (IP) and the adequacy of anesthesia was monitored by the disappearance of the pedal withdrawal reflex [14]. After incubation with PE-90 tubing and ventilation using a mouse miniventilator with air, surgical procedures were initiated and the left coronary artery (LCA) was ligated (no ligation for sham) for 30 min followed by 120 min of reperfusion as previously described [15]. The drug was directly dissolved in 1 ml NS in 37°C as described elsewhere [16] and administrated by IP. The same amount of NS was administrated in sham mice. In the indicated time points, the mice were sacrificed by overdose anesthesia with pentobarbital sodium (150 mg/kg, IP) and cervical dislocation, and the hearts were extracted for further analysis.

PD used in this study is an injection developed by Neptunus Co., Ltd (Shenzhen, China) which can be applied after diluted with normal saline (NS). 3-methyladenine (3-MA) was purchased from Sigma-Aldrich Company.

We designed the following groups: Sham group; I/R + NS group; I/R + PD group; I/R + PD + 3-MA group (15 mg/kg of 3-MA); I/R + 3-MA group.

Cardiomyocyte culture and cell viability assay

Neonatal rat cardiomyocytes (NRCs) were isolated from 1–3 day Sprague-Dawley rats and cultured as previously described [26]. To mimic an *in vivo* I/R model, H/R treatments were used. Cells were washed with PBS and incubated in complete-medium or starvation medium (lacking amino acids and serum) for 3 h at 37°C in a hypoxic chamber (Modular Incubator Chamber) equilibrated with 95% N_2 and 5% CO_2. Reoxygenation was then initiated by buffer exchange to normoxic complete medium alone or supplemented with 1, 10 or 100 μM PD.

Cell viability was measured by MTS assay (Promega) according to the manufacturer's instructions. Briefly, after drug administration, NRCs were treated with MTS and incubated for 4 h at 37°C in the dark. Absorbance was then measured at 490 nm using a microplate reader (Bio-Rad) and readings were normalized with vehicle control. NRCs were exposed to 3 h hypoxia/3 h re-oxygenation with or without PD,

3-MA (10 mM), Bafilomycin A1 (Baf, 100 nM) (Sigma-Aldrich) and MnTMPyP (50 μM, Merck Millpore). In some experiments, NRCs were pretreated with 10 mM N-acetylcysteine (NAC) (Sigma-Aldrich) for 1 h before exposure to H/R. Cells were harvested for analysis after 3 h reoxygenation.

Apoptosis assay

Apoptosis was analyzed using TUNEL (Invitrogen) assay according to the manufacturer's instructions. Apoptotic nucleuses were visualized with light microscopy or fluorescent microscopy. TUNEL-stained cell (%) was calculated according to the distribution of myocardial cells under microscopy (×100), five views were chosen in each section, and 200 cells were counted in each view, then calculated the average percentage of apoptotic cell as apoptosis index.

Western blot

Samples were obtained from NRCs or mouse hearts. Protein concentrations were measured via a BCA method (Promega), and equal amounts of protein were resolved via SDS-PAGE and transferred to PVDF membranes (Millipore). After blocking in 5% non-fat milk at room temperature for 2 h, membranes were incubated with the following primary antibodies overnight at 4°C: anti-cleaved caspase-3 (Asp175), anti-LC3B, anti-p62 (all from Cell Signaling Technology) and anti-GAPDH (Kangchen). All dilutions were 1:1000. After incubation for 2 h at room temperature with secondary antibodies (Boster), the bands were visualized using enhanced chemiluminescence (Millipore). The blots were quantified by densitometry using Image-Pro-Plus 6.0 software (Media Cybernetic) and the relative protein expression was compared with GAPDH.

Transmission Electron Microscopy (TEM)

Small fragments of myocardium sized ~1 mm^3 and NRCs were fixed overnight by immersion in 2.5% glutaraldehyde, 0.01% picric acid, 0.1 M cacodylate buffer, pH 7.4. After rinsed in the same buffer, the tissues were immersed in 1% osmium tetroxide in 0.1 M cacodylate buffer for 1 h followed by block incubation with 2% aqueous uranyl acetate for 2 h. The samples were dehydrated with a graded series of ethanol (50%, 70%, 90%, 100%), propylene oxide and then infiltrated with a 1:1 mixture of propylene oxide and EMbed 812 (Electron Microscopy Sciences). Ultrathin sections (75–80 nm) were cut with ultramicrotome, collected on 200-mesh copper grids and contrasted with in 5% uranyl acetate in ethanol (10 min) and lead citrate (5 min). Grids were examined with a Philips CM 10 electron microscope operated at 80 kV.

Myocardial infarct size measurement

2, 3, 5-triphenyltetrazolium chloride (TTC) and Evans blue dye were used to detect myocardial infarct size as previously described [10] with minor modifications. After reperfusion, the ligature was re-tightened and 0.25% Evans blue was injected to stain the normally perfused region of the heart. The heart was then frozen and cut into 2-mm slices, which were stained with TTC at 37°C for 20 min. The area stained with Evans blue represented the non-I/R myocardium, whereas the unstained area was the I/R myocardium, or area at risk (AAR). Within the AAR, I/R but viable myocardium stained brick red by TTC, whereas dead myocardium (infarct) was white. The infarct size was calculated as IS/AAR (%). For sham-operated hearts, the thread was passed around the LCA but left untied during I/R period. Prior to the AAR was detected, the LCA was occluded before Evans blue infusion after thoracotomy and threading. Therefore, the Evans blue doesn't enter the LCA perfused myocardium. Then TTC staining was used to evaluate the infarct size in sham-operated hearts. Images were captured using a camera and the area of the infarcted myocardium was analyzed with Image Pro-plus 6.0 software.

Echocardiography

Cardiac function was evaluated by non-invasive transthoracic echocardiography using a Visual Sonics Vevo 770 system with a RMV707B probe (Visual Sonics) 7 days after surgery. Mice were anesthetized using 2% isoflurane, and the left chest was denuded. M-mode echocardiographic views of the mid-ventricular short axis were obtained at the level of the papillary muscle tips below the mitral valve [17]. The left ventricular end-diastolic (Did) and systolic (Dis) diameter, end-diastolic (Vid) and systolic dimension (Vis) were measured. Left ventricular fractional shortening (LVFS) and ejection fraction (EF) were calculated as follows:

$$LVFS\ (\%) = (Did - Dis) / Did \times 100$$

$$EF\ (\%) = (Vid - Vis) / Vid \times 100$$

Adenovirus-short hairpin RNA of Beclin 1(Ad-sh-Beclin 1) infection

Ad-sh-Beclin 1 and Ad-negative control (Ad-NC) were generated by a professional company (Vigene Biosciences). NRCs were cultured for 3 days, then directly transfected with the Ad-sh-Beclin 1 or Ad-NC [13]. Multiplicity of infection (MOI) was 10 and the transduction efficiency exceeded 90%.

Evaluation of fluorescent LC3 puncta

NRCs cultured on coverslips were transfected with adenovirus of tandem fluorescent mRFP-GFP-LC3 (MOI = 15). Twenty-four hours after adenoviral transfection, cells were washed with PBS, fixed with 4% paraformaldehyde, mounted with a reagent containing 4, 6-diamidino-2-phenylindole (DAPI) (Sigma-Aldrich), and viewed under a confocal laser scanning microscopy (OLYMPUS FV1000). Punctuate localization of LC3 on autophagosomes had both red and green fluorescence and appeared yellow in merged images due to autophagosome induction. Subsequently, GFP instability in the acidic lysosomal compartment leads to loss of the green fluorescent signal on fused autophagosome-lysosomes and formation of autolysosomes [18]. Therefore, red dots that do not overlay green dots and appear red in merged images indicate autolysosome formation. The transfection efficiency was more than 90%, and the subsequent transfection-induced cell death was less than 10%.

Measurement of mitochondrial membrane potential (ΔΨm)

ΔΨm was estimated using a commercial kit (Beyotime) as described elsewhere [19]. Briefly, after treatment, cells were incubated with the JC-1 staining solution (5 μg/ml) for 20 min at 37°C, and then washed three times with JC-1 staining buffer and assayed with confocal laser scanning microscopy (OLYMPUS FV1000, λ_{ex} 488 nm; λ_{em} 530 and 590 nm). ΔΨm was determined by the red/green ratio. Rhodamine 123 (Sigma-Aldrich) also was used for ΔΨm detection in accordance with the manufacturer's instructions. Briefly, NRCs were washed and incubated with Rhodamine 123 (1 μM) for 30 min after experimental manipulations, then they were trypsinized and flow cytometry was used to assay cells with emission in the FL1 channel (BD, FACS Calibur). FlowJo software was used for analysis.

Intracellular reactive oxygen species (ROS) measurements

Intracellular ROS was quantified with 2,7-dichlorofluoresein diacetate (DCFH-DA) (Sigma-Aldrich) [20]. Confocal laser scanning microscopy (OLYMPUS FV1000) and flow cytometer (BD, FACS Calibur) were used to detect assay. For fluorescent microscopy analysis, NRCs were seeded in laser confocal petri dishes, incubated with culture medium containing 20 μM DCFH-DA for 30 min at 37°C and washed three times with PBS. Then, cells were visualized microscopically (λex 488 nm, λem 525 nm). For flow cytometry, NRCs were cultured in 6-well flat-bottom tissue culture plates, treated and incubated with 20 μM DCFH-DA for 30 min at 37°C, then washed and trypsinized and subjected to flow cytometry with emission in the FL1 channel. FlowJo software was used for analysis. NRCs treated with 150 μM H_2O_2 for 2 h was used as positive control

[18].

Measurement of hydrogen peroxide (H_2O_2)

H_2O_2 was determined with an Amplex red hydrogen peroxide assay kit (Molecular Probes) according to the manufacturer's instructions. Briefly, the harvested NRCs after treatments were lysed by three cycles of freeze-thawing [21]. The supernatant collected after centrifugation was reacted with Amplex red (100 μM) and horseradish peroxidase (0.2 U/ml) in 96-well plates for 30 min at room temperature. The absorbance was determined spectrophotometrically (Molecular Devices) at 560 nm. The results were expressed as micromoles per gram of protein.

Quantitation of superoxide anion release

Superoxide anion production was determined by using the superoxide dismutase–inhibitable (SOD-inhibitable) cytochrome c reduction assay as previously described [21]. Briefly, 500 μl culture media were mixed with 50 μl cytochrome c (40 μM, Sigma-Aldrich), followed by adding 250μl Hank's balanced salt solution. The mixtures were incubated at room temperature for 10 min with or without 50μl SOD (100 μg/ml, Sigma-Aldrich). The absorbance was measured spectrophotometrically at 550 nm. The extinction coefficient for reduced cytochrome c is 21,000 mM/cm and the calculated results were expressed as micromoles per gram of protein.

Statistical analysis

All analyses were performed using SPSS 17.0 software. All data were expressed as means ± standard error of the mean (SEM) and $P < 0.05$ was considered to be statistically significant. Statistical differences were evaluated using one-way ANOVA followed by Bonferroni's or Dunnett's T3 multiple comparison exact probability tests.

RESULTS

Effects of PD on cardiomyocyte apotosis and signatures of autophagy and apoptosis

In cultured NRCs exposed to H/R, PD (1, 10, 100 μM) dose-dependently improved cell survival, but there was no significant difference between 10 μM and 100 μM groups (Fig. 1B). Thus, 10 μM of PD was applied in subsequent *in vitro* experiments. In mice insulted with I/R, TUNEL assay showed that PD (5, 7.5, 10 mg/kg) dose-dependently decreased apoptosis, but there was no significant difference between the 7.5 and 10 mg/kg

groups (Fig.1C and D). Therefore, the concentration of 7.5 mg/kg was chosen for subsequent *in vivo* experiments.

In NRCs exposed to H/R, western blot showed that 1 and 10 μM of PD significantly up-regulated LC3 II and down-regulated p62 as well as cleaved caspase-3, but 100 μM of PD significantly decreased LC3 (Fig. 1E). Similar results were found in I/R mice treated with PD or NS (Fig. 1F).

PD-induced autophagy decreased myocardial apoptosis *in vivo* and *in vitro*

In mice subjected to I/R, PD increased LC3 II/I and LC3 II and decreased cleaved caspase-3, and these effects were abrogated by co-treatment with 3-MA, that inhibits class III PI3K activity [22] (Fig. 2A). Similar results also were noted in NRCs exposed to H/R (Fig. S1A). Next, Ad-sh-Beclin 1 was applied to NRCs. After 24 h infection, the transduction efficiency was over 90% (Fig. 2B). Beclin 1 was reduced by about 70% in the Ad-sh-Beclin 1 treated cardiomyocytes (Fig 2C). In NRCs exposed to H/R, co-treatment with Ad-sh-Beclin 1 led to a significantly lower LC3 II/I protein ratio and LC3 II/GAPDH in H/R group and H/R+PD group, respectively (Fig. 2D, E). MTS assay indicated that Ad-sh-Beclin 1 decreased the viability of NRCs with or without H/R treatment, while the effect of PD reducing cell loss responsed to H/R was abolished by co-treatment with Ad-sh-Beclin 1(Fig 2F). And TUNEL assay revealed that cell death was increased in the H/R group compared with control, and the effect of PD on decreasing cell death was partly blocked by 3-MA (Fig. S1B, C).

PD reduced myocardial infarct size and improved heart function in I/R mice

To examine the efficacy of PD post-treatment on I/R injury, myocardial cell ultrastructure was examined by TEM. Numerous dense and tight mitochondria, and neatly arranged and intact myocardial fibrils could be seen in the cytoplasm of sham group. In contrast, I/R-treated group had loose and swollen mitochondria with ruptured or disappearing swollen myocardial fibrils (Fig. 3A). Cardiomyocytes in PD treated mice had less pathological changes: less ruptured mitochondria and myocardial fibrils, and more highly visible vacuoles with/without content, while I/R-induced mitochondrial swelling was alleviated by PD as evidenced by decreased mitochondrial mean area (Fig. 3A).

The infarct size in I/R + PD group was significantly reduced in comparison with I/R group (59 ± 4.5% vs. 30 ± 4.0%; Fig. 3B, C), while co-treatment with 3-MA abrogated the effect of PD on reducing myocardial infarct size (42 ± 2.8% vs. 30 ± 4.0%) (Fig. 3B, C). There

were no significant differences in AAR/LV among the groups (Fig. 3B, D).

Two-D and M-mode of Echocardiographic examinations were performed (Fig. 3E and F). LVFS and EF were significantly lower in I/R group than in the sham group, which were improved by PD post-treatment, while autophagic inhibitor 3-MA blunts this beneficial effect by PD post-treatment (Fig. 3G, H).

PD enhanced autophagic flux in NRCs exposed to H/R

To monitor autophagic flux, tandem fluorescent mRFP-GFP-LC3 was performed on NRCs (Ad-LC3-NRCs). The normal Ad-LC3-NRCs had basal autophagy with few autolysosomes and few autophagosomes (Fig. 4A and B). Ad-LC3-NRCs subjected to H/R had accumulated autophagosomes and few autolysosomes (Fig. 4A and B), suggesting that autophagosome clearance was inhibited and autophagic flux was blocked or impaired during myocardial H/R. In PD-treated group, Ad-LC3-NRCs subjected to H/R had more autolysosomes and less autophagosomes than in untreated group (Fig. 4A and B), indicating PD treatment induces the consumption of autophagosomes and enhanced autophagic flux. However, co-treatment with PD and autophagic inhibitor 3-MA decreased autolysosomes compared with PD. In addition, data showed that the ratio of LC3 II/I and LC3 II had no significant difference between H/R groups present and absent of Baf (a lysosomal inhibitor), while co-treatment with Baf and PD induced the accumulation of LC3 II in NRCs exposed to H/R (Fig. 4C), indicating that PD promoted the degradation of autolysosome. Thus, autophagosomes accumulated may be due to impaired autophagy during H/R, and PD treatment induced a significant clearance of autophagosomes with the degradation of autolysosome. TUNEL assay indicated that PD post-treatment decreased the apoptosis of NRCs exposed to H/R, while Baf partly abolished this effect of PD (Fig. 4D).

PD-induced autophagic flux attenuated mitochondria damage

TEM examination showed that NRCs in H/R+PD group produced more autolysosomes than in H/R group, indicating that PD can lead a shift from early autophagic vacuoles to late autolysosomes, while the effect of PD was partly abolished by 3-MA (Fig.5A). $\Delta\Psi m$ was dramatically reduced in NRCs exposed to H/R, and partially restored by PD. However, the effect of PD was abolished by Baf (Fig. 5B, C).

PD-induced autophagic flux reduced cellular ROS

As damaged mitochondria are the major source of ROS production, we investigated effects of PD on cellular ROS production in NRCs. Exposing NRCs to H/R significantly increased nonspecific ROS production. And

PD markedly inhibited ROS production (Fig. 6A-B). However, the inhibitory effect of PD on ROS generation was blocked by Baf (Fig. 6A-B).

In addition, to confirm whether PD post-treatment had effects on H_2O_2, NRCs were quantified using Amplex red assay. H_2O_2 was significantly increased in the H/R group compared with control, and the effect of PD on decreasing H_2O_2 was partly eliminated by Baf (Fig. 6C). Similar results were also found by quantifying with SOD-inhibitable cytochrome c reduction assay to detect superoxide anion (Fig. 6D). These results showed that PD-induced autophagic flux reduced the generation of H_2O_2 and superoxide anions.

DISCUSSION

This study indicates that PD treatment during reperfusion exerts significant protective effects against myocardial I/R injury by enhancing autophagic flux. We illustrated the major findings in Figure 7. PD post-treatment promotes autophagic flux to clear damaged mitochondria to reduce ROS and cell death, and thus limits myocardial infarct size.

Previous studies suggest that autophagy is increased in mouse heart during both ischemia and reperfusion [23, 24], while the effect of autophagy on myocardial I/R injury is controversial and may be context-dependent. Some researchers have proposed that whether up-regulation of autophagy is beneficial or detrimental may depend on the extent of autophagy. Moderate autophagy is reported to be beneficial for cardiomyocyte survival but excessive autophagy exacerbates cardiomyocyte death [13, 25]. Sadoshima's group reported that autophagy was amplified during reperfusion and exacerbated cardiomyocyte death after ischemia, suggesting that excessive autophagy was detrimental to the heart [24]. In our study, the protective effects of PD may be attributed to enhanced autophagic flux. Our tandem fluorescent mRFP-GFP-LC3 results indicate that autophagosomes were accumulated and autophagic flux was impaired during H/R, while PD induced autophagosome clearance. Consistent with our data, a study revealed that autophagic flux was impaired at the phase of autophagosome-lysosome fusion as well as autolysosome degradation during reperfusion, which did not show protective effects against myocardial cell death during I/R injury [18]. And this phenomenon highlighted the importance of identifying "intact autophagic flux" to accurately characterize autophagy, which is a dynamic process.

Given that undigested autophagosome and damaged mitochondria may release harmful substances such as ROS to aggravate cell death [18],

elimination of damaged mitochondria and autophagosomes would prevent further injury to neighboring mitochondria and the wholesale opening of mitochondrial permeability transition pore [26]. Our results indicate that ΔΨm was decreased and ROS was increased in myocardial cells exposed to H/R, while ΔΨm was restored and ROS production was inhibited by PD post-treatment. Enhanced myocardial cell viability by PD may result from fewer damaged mitochondria and production of less ROS.

PD exerts anti-oxidant effects by increasing superoxide dismutase expression which is an anti-oxidant enzyme [5]. The partial restoration of ROS production after co-treatment with autophagic inhibitor and PD suggested that the protective effects of PD were associated with scavenging ROS. Our results have confirmed that PD reduced the generation of H_2O_2 and superoxide anions. This is consistent with a recent study reported that PD pre-treatment exerted cardioprotective effects via eliminating free oxidative radical [10].

Inflammation plays a significant role in myocardial I/R injury [27] and it is involved not only in acute tissue damage, but also in subsequent tissue repair and healing [28]. Monocyte/macrophage infiltration after myocardial infarction has been confirmed, suggesting that inhibition of excessive inflammation could limit infarct size and strengthen heart function [29]. Studies have confirmed that PD has anti-inflammatory effects via inhibiting expression of interleukin-17 [30] and various cell adhesion molecules [31]. And our data revealed that PD decreased polymorphonuclear leukocytes (PMNs) in mice exposed to I/R (Fig. S2). Thus, the cardioprotection of PD found in this study may depend on multiple mechanisms, including scavenging ROS, eliminating damaged mitochondria, promoting autophagosome clearance and restricting inflammation.

Apoptosis may be indirectly regulated by autophagy via alleviating ROS production. Two major mechanisms activate caspases: the extrinsic pathway which activates caspase-8 and the intrinsic pathway or the mitochondrial-dependent mechanism which activates caspase-9. Both pathways activate executioner caspase-3. Kamata etc. reported that reduction of ROS accumulation deactivated the extrinsic pathway and promoted cell survival by transiently activating JNK [32]. In regard to the mitochondria-dependent mechanism, pro-apoptotic Bcl-2 family proteins cause transient mitochondrial permeability transition pore opening, which promotes ROS accumulation [33] and Bax- or Bak-mediated outer mitochondrial membrane permeabilization along with subsequent generation of ROS [34]. Consequently, it facilitates the release of mitochondrial-resident apoptogenic factors (such as cytochrome *c*) [35] and these activities ultimately lead to apoptotic cell death. As cytochrome

c triggers a post-mitochondrial pathway forming “apoptosome” of cytochrome c, Apaf-1 and caspase-9, which subsequently cleaves the effector caspases -3 and -7 [35, 36], the deficiencies of cytochrome c display defects in apoptosis following intrinsic signals [37]. Therefore, promoting autophagic flux and anti-oxidative action by PD to reduce ROS production may decrease apoptosis through the above-mentioned mechanisms.

The smooth process of autophagic flux accompanied by the attenuation of apoptotic cell death after PD treatment and the upregulation of apoptosis induced by autophagic inhibitor highlight the role of autophagy in apoptotic regulation. It was reported that inhibiting autophagy triggered apoptosis [38], and that the up-regulation of autophagy protected cardiac tissue against apoptotic stimuli [39]. Furthermore, autophagy was reported not only to degrade damaged mitochondria and cleave caspases such as caspase-3, but also to provide a membrane-based intracellular platform to process caspases during apoptotic regulation [40]. Our findings suggest that up-regulation of autophagy by PD is accompanied with reduced apoptosis and the administration of autophagic inhibitor disturbs optimal autophagy and leads to apoptosis. In addition, a previous study revealed that autophagy and apoptosis could be cooperative or competitive pathways depending on the cellular environment [41]. However, the mechanisms of cross-talks between autophagy and apoptosis remain unclear and should be explored in future studies.

CLINICAL PERSPECTIVES

- PD pre-treatment has cardioprotective effects, but the effects of PD post-treatment and its underlying mechanisms during I/R are unknown.
- This paper provides evidence that PD post-treatment promotes autophagic flux to clear damaged mitochondria to reduce ROS and cell death, and thus limits infarct size.
- The findings in this study suggest that PD post-treatment is likely to be an alternative strategy to attenuate myocardial I/R injury in patients with MI.

AUTHOR CONTRIBUTION

This study was conceived and designed by Aihua Chen, Yuanna Ling, Xianbao Wang, and Guiming Chen. Data and results were analyzed and interpreted by Yuanna Ling, Aihua Chen, Xianbao Wang, Yulin Liao,

Masafumi Kitakaze, Guiming Chen, Yi Deng, Huixiong Tang, Long Ling, Xiaoming Zhou, Xudong Song, and Pingzhen Yang. Experiments were performed by Yuanna Ling, Guiming Chen, Xianbao Wang and Yi Deng. The manuscript was written, edited, and revised by Yuanna Ling, Yulin Liao, Aihua Chen, Masafumi Kitakaze, Xianbao Wang, Guiming Chen.

ACKNOWLEDGE

We are grateful to Dr. Yan Wang (Institute of Regenerative Medicine, Zhujiang Hospital, Southern Medical University, China) for generosity in sharing valuable technical assistance and laboratory equipment and Professor Kesen Zhao (Department of pathophysiology, Southern Medical University, China) for the generous gift of PD.

FUNDING

This work was supported by grants from the National Natural Science Foundation of China (81270218, to Prof. Chen), and National Natural Science Foundation of China (81400190, to Dr. Wang).

REFERENCES

1 Sanada, S., I. Komuro, and M. Kitakaze. (2011) Pathophysiology of myocardial reperfusion injury: preconditioning, postconditioning, and translational aspects of protective measures. American journal of physiology. Heart and circulatory physiology. **301**, H1723-1741

2 Luo, T., B. Chen, Z. Zhao, N. He, Z. Zeng, B. Wu, Y. Fukushima, M. Dai, Q. Huang, D. Xu, J. Bin, M. Kitakaze, and Y. Liao. (2013) Histamine H2 receptor activation exacerbates myocardial ischemia/reperfusion injury by disturbing mitochondrial and endothelial function. Basic research in cardiology. **108**, 342

3 Basalay, M., V. Barsukevich, S. Mastitskaya, A. Mrochek, J. Pernow, P.O. Sjoquist, G.L. Ackland, A.V. Gourine, and A. Gourine. (2012) Remote ischaemic pre- and delayed postconditioning - similar degree of cardioprotection but distinct mechanisms. Exp. Physiol. **97**, 908-917

4 Ravagnan, G., A. De Filippis, M. Carteni, S. De Maria, V. Cozza, M. Petrazzuolo, M.A. Tufano, and G. Donnarumma. (2013) Polydatin, a natural precursor of resveratrol, induces beta-defensin production and reduces inflammatory response. Inflammation. **36**, 26-34

5 Ji, H., X. Zhang, Y. Du, H. Liu, S. Li, and L. Li. (2012) Polydatin modulates inflammation by decreasing NF-kappaB activation and oxidative stress by increasing Gli1, Ptch1, SOD1 expression and ameliorates blood-brain barrier permeability for its neuroprotective effect in pMCAO rat brain. Brain Research Bulletin. **87**, 50-59

6 Gao, J.P., C.X. Chen, W.L. Gu, Q. Wu, Y. Wang, and J. Lu. (2010) Effects of polydatin on attenuating ventricular remodeling in isoproterenol-induced mouse and pressure-overload rat models. Fitoterapia. **81**, 953-960

7 Dong, M., W. Ding, Y. Liao, Y. Liu, D. Yan, Y. Zhang, R. Wang, N. Zheng, S. Liu, and J. Liu. (2015)

Polydatin prevents hypertrophy in phenylephrine induced neonatal mouse cardiomyocytes and pressure-overload mouse models. Eur. J. Pharmacol. **746**, 186-197

8 Romero-Pérez, A.I., M. Ibern-Gómez, R.M. Lamuela-Raventós, and M.C. de la Torre-Boronat. (1999) Piceid, the Major Resveratrol Derivative in Grape Juices. J. Agric. Food Chem. **47**, 1533-1536

9 Hung, L.M., M.J. Su, and J.K. Chen. (2004) Resveratrol protects myocardial ischemia-reperfusion injury through both NO-dependent and NO-independent mechanisms. Free Radic. Biol. Med. **36**, 774-781

10 Miao, Q., S. Wang, S. Miao, J. Wang, Y. Xie, and Q. Yang. (2011) Cardioprotective effect of polydatin against ischemia/reperfusion injury: roles of protein kinase C and mito K(ATP) activation. Phytomedicine. **19**, 8-12

11 Galluzzi, L., F. Pietrocola, B. Levine, and G. Kroemer. (2014) Metabolic Control of Autophagy. Cell. **159**, 1263-1276

12 Gurusamy, N., I. Lekli, S. Mukherjee, D. Ray, M.K. Ahsan, M. Gherghiceanu, L.M. Popescu, and D.K. Das. (2010) Cardioprotection by resveratrol: a novel mechanism via autophagy involving the mTORC2 pathway. Cardiovasc. Res. **86**, 103-112

13 Xu, Q., X. Li, Y. Lu, L. Shen, J. Zhang, S. Cao, X. Huang, J. Bin, and Y. Liao. (2015) Pharmacological modulation of autophagy to protect cardiomyocytes according to the time windows of ischaemia/reperfusion. British Journal of Pharmacology. **172**, 3072-3085

14 Chen, B., D. Lu, Y. Fu, J. Zhang, X. Huang, S. Cao, D. Xu, J. Bin, M. Kitakaze, Q. Huang, and Y. Liao. (2014) Olmesartan prevents cardiac rupture in mice with myocardial infarction by modulating growth differentiation factor 15 and p53. Br. J. Pharmacol. **171**, 3741-3753

15 Zhou, S.S., F. He, A.H. Chen, P.Y. Hao, and X.D. Song. (2012) Suppression of rat Frizzled-2 attenuates hypoxia/reoxygenation-induced Ca2+ accumulation in rat H9c2 cells. Exp. Cell Res. **318**, 1480-1491

16 Wang, X., R. Song, Y. Chen, M. Zhao, and K.S. Zhao. (2013) Polydatin--a new mitochondria protector for acute severe hemorrhagic shock treatment. Expert opinion on investigational drugs. **22**, 169-179

17 Zeng, Z., L. Shen, X. Li, T. Luo, X. Wei, J. Zhang, S. Cao, X. Huang, Y. Fukushima, J. Bin, M. Kitakaze, D. Xu, and Y. Liao. (2014) Disruption of histamine H2receptor slows heart failure progression through reducing myocardial apoptosis and fibrosis. Clin. Sci. **127**, 435-448

18 Ma, X., H. Liu, S.R. Foyil, R.J. Godar, C.J. Weinheimer, J.A. Hill, and A. Diwan. (2012) Impaired autophagosome clearance contributes to cardiomyocyte death in ischemia/reperfusion injury. Circulation. **125**, 3170-3181

19 Wang, S., Y. Li, X. Song, X. Wang, C. Zhao, A. Chen, and P. Yang. (2015) Febuxostat pretreatment attenuates myocardial ischemia/reperfusion injury via mitochondrial apoptosis. J. Transl. Med. **13**, 209

20 Wang, H. and J.A. Joseph. (1999) Quantifying cellular oxidative stress by dichlorofluorescein assay using microplate reader. Free Radical Biol. Med. **27**, 612-616

21 Sun, H.Y., N.P. Wang, F. Kerendi, M. Halkos, H. Kin, R.A. Guyton, J. Vinten-Johansen, and Z.Q. Zhao. (2005) Hypoxic postconditioning reduces cardiomyocyte loss by inhibiting ROS generation and intracellular Ca2+ overload. Am. J. Physiol. Heart Circ. Physiol. **288**, H1900-1908

22 Wu, Y.T., H.L. Tan, G. Shui, C. Bauvy, Q. Huang, M.R. Wenk, C.N. Ong, P. Codogno, and H.M.

Shen. (2010) Dual role of 3-methyladenine in modulation of autophagy via different temporal patterns of inhibition on class I and III phosphoinositide 3-kinase. J. Biol. Chem. **285**, 10850-10861

23 Hamacher-Brady, A., N.R. Brady, and R.A. Gottlieb. (2006) Enhancing macroautophagy protects against ischemia/reperfusion injury in cardiac myocytes. J. Biol. Chem. **281**, 29776-29787

24 Matsui, Y., H. Takagi, X. Qu, M. Abdellatif, H. Sakoda, T. Asano, B. Levine, and J. Sadoshima. (2007) Distinct roles of autophagy in the heart during ischemia and reperfusion: roles of AMP-activated protein kinase and Beclin 1 in mediating autophagy. Circ. Res. **100**, 914-922

25 Lavandero, S., R. Troncoso, B.A. Rothermel, W. Martinet, J. Sadoshima, and J.A. Hill. (2013) Cardiovascular autophagy: concepts, controversies, and perspectives. Autophagy. **9**, 1455-1466

26 Gottlieb, R.A. and A.B. Gustafsson. (2011) Mitochondrial turnover in the heart. Biochim. Biophys. Acta. **1813**, 1295-1301

27 Wang, C., H. Sun, Y. Song, Z. Ma, G. Zhang, X. Gu, and L. Zhao. (2015) Pterostilbene attenuates inflammation in rat heart subjected to ischemia-reperfusion: role of TLR4/NF-κB signaling pathway. Int. J. Clin. Exp. Med. **8**, 1737-1746

28 Frantz, S., J. Bauersachs, and G. Ertl. (2009) Post-infarct remodelling: contribution of wound healing and inflammation. Cardiovasc. Res. **81**, 474-481

29 Rohrbach, S., C. Troidl, C. Hamm, and R. Schulz. (2015) Ischemia and reperfusion related myocardial inflammation: A network of cells and mediators targeting the cardiomyocyte. IUBMB life. **67**, 110-119

30 Lanzilli, G., A. Cottarelli, G. Nicotera, S. Guida, G. Ravagnan, and M.P. Fuggetta. (2012) Anti-inflammatory effect of resveratrol and polydatin by in vitro IL-17 modulation. Inflammation. **35**, 240-248

31 Cheng, Y., H.T. Zhang, L. Sun, S. Guo, S. Ouyang, Y. Zhang, and J. Xu. (2006) Involvement of cell adhesion molecules in polydatin protection of brain tissues from ischemia-reperfusion injury. Brain Res. **1110**, 193-200

32 Kamata, H., S.-i. Honda, S. Maeda, L. Chang, H. Hirata, and M. Karin. (2005) Reactive Oxygen Species Promote TNFα-Induced Death and Sustained JNK Activation by Inhibiting MAP Kinase Phosphatases. Cell. **120**, 649-661

33 Hagenbuchner, J., A. Kuznetsov, M. Hermann, B. Hausott, P. Obexer, and M.J. Ausserlechner. (2012) FOXO3-induced reactive oxygen species are regulated by BCL2L11 (Bim) and SESN3. J. Cell Sci. **125**, 1191-1203

34 Wei, M.C., T. Lindsten, V.K. Mootha, S. Weiler, A. Gross, M. Ashiya, C.B. Thompson, and S.J. Korsmeyer. (2000) tBID, a membrane-targeted death ligand, oligomerizes BAK to release cytochrome c. Genes Dev. **14**, 2060-2071

35 Scorrano, L., K. Ashiya M Fau - Buttle, S. Buttle K Fau - Weiler, S.A. Weiler S Fau - Oakes, C.A. Oakes Sa Fau - Mannella, S.J. Mannella Ca Fau - Korsmeyer, and S.J. Korsmeyer. (2002) A distinct pathway remodels mitochondrial cristae and mobilizes cytochrome c during apoptosis. Dev. Cell. **2**, 55-67

36 Scorrano, L. and S.J. Korsmeyer. (2003) Mechanisms of cytochrome c release by proapoptotic BCL-2 family members. Biochem. Biophys. Res. Commun. **304**, 437-444

37 Li, K., Y. Li, J.M. Shelton, J.A. Richardson, E. Spencer, Z.J. Chen, X. Wang, and R.S. Williams.

Cytochrome c Deficiency Causes Embryonic Lethality and Attenuates Stress-Induced Apoptosis. Cell. **101**, 389-399

38 Boya, P., R.A. Gonzalez-Polo, N. Casares, J.L. Perfettini, P. Dessen, N. Larochette, D. Metivier, D. Meley, S. Souquere, T. Yoshimori, G. Pierron, P. Codogno, and G. Kroemer. (2005) Inhibition of macroautophagy triggers apoptosis. Mol. Cell. Biol. **25**, 1025-1040

39 Ravikumar, B., Z. Berger, C. Vacher, C.J. O'Kane, and D.C. Rubinsztein. (2006) Rapamycin pre-treatment protects against apoptosis. Hum. Mol. Genet. **15**, 1209-1216

40 Mukhopadhyay, S., P. Panda, N. Sinha, D. Das, and S. Bhutia. (2014) Autophagy and apoptosis: where do they meet? Apoptosis. **19**, 555-566

41 Vitale, N., A. Kisslinger, S. Paladino, C. Procaccini, G. Matarese, G.M. Pierantoni, F.P. Mancini, and D. Tramontano. (2013) Resveratrol couples apoptosis with autophagy in UVB-irradiated HaCaT cells. PLoS One. **8**, e80728

FIGURE LEGENDS

Figure 1 Effects of PD on cardiomyocyte apotosis and signatures of autophagy and apoptosis.

(A) Chemical structures of PD and RES. **(B)** Effects of different doses of PD (1, 10 and 100 μM PD) on MTS-assay determined cell viability in cultured NRCs. $^{*}P < 0.05$ vs. control group, $^{\#}P < 0.05$ vs. H/R group. Effects of different doses of PD (5, 7.5, 10 mg/kg) on cardiomyocytes apoptosis in mice subjected to I/R also were evaluated. Apoptotic cells were visualized using TUNEL staining (brown nuclei) **(C)** and quantitatively analyzed **(D)**. $^{*}P < 0.01$ vs. sham group, $^{\#}P < 0.05$ vs. I/R group. Western blots of LC3, p62 and cleaved caspase-3 in NRCs under H/R **(E)** and in murine hearts subjected to I/R **(F)**, and the quantification of the LC3 II/I ratio**,** LC3 II/GAPDH**,** p62/GAPDH and cleaved caspase-3/GAPDH were showed. $^{*}P < 0.05$ vs. the corresponding control or sham group, $^{\#}P < 0.05$ vs. H/R or I/R + NS group, $^{\&}P < 0.05$ vs. PD 10 μM or PD 7.5 mg/kg group. Values are expressed as mean ± SEM. *In vitro* experiments were repeated 3-4 times. For panel **D** and **F,** $n = 5$ of each group. PD, polydatin; Res, resveratrol; C, control; H/R, hypoxia/reoxygenation; I/R, ischemia/reperfusion.

Figure 2 PD-induced autophagy decrease myocardial apoptosis *in vivo* and *in vitro*

(A) Western blots of LC3 and cleaved caspase-3 in different groups, n = 5, $^{*}P < 0.05$ vs. Sham group, $^{\#}P < 0.05$ vs. I/R + NS group, $^{\S}P < 0.05$ vs. I/R + PD group, $^{\&}P < 0.05$ vs. I/R + PD + 3-MA group. **(B)** Infective efficiency of adenovirus carrying short hairpin RNA for Beclin 1 (Ad-sh-Beclin 1) and negative control (Ad-sh-NC) in NRCs after 24 h infection. **(C)** Silencing effect of Beclin 1 was confirmed using Western blot. **(D)** Western blot of LC3 expression in different groups with or without sh-beclin 1 co-treatment. **(E)** Quantification for panel D. **(F)** Cell viability was determined by MTS assay. Experiments were repeated for three times, and data were expressed as means ± SEM. $^{*}P < 0.05$ vs. C+sh-NC group, $^{\#}P < 0.05$ vs. H/R+sh-NC group. $^{\&}P < 0.05$ vs. H/R+PD+sh-NC group. I/R, ischemia/reperfusion; NS, normal saline; PD, polydatin; 3-MA, 3-methyladenine; MOI, multiplicity of infection; GFP, green fluorescent protein; sh, short hairpin RNA; NC, negative control; B, beclin 1; C, control; H/R,

hypoxia/reoxygenation.

Figure 3 Effects of PD post-treatment on mitochondrial damage, infarct size and heart function in mice subjected to I/R

Mice in this experiment were treated with 7.5 mg/kg PD or 15 mg/kg 3-MA during reperfusion. **(A)** The ultrastructure of cardiomyocytes in different groups was showed in TEM pictures. m, mitochondria; yellow arrow, vacuoles packed with or without contents. Early autophagic vacuoles packed with contents **(a,b)** and autolyosomes containing degradation products **(c,d)** in myocardium of PD treatment group were shown ; And the mean mitochondrial area in different groups were shown in the bar graph (n = 4 of each group). **(B)** Representative TTC-Evans blue stained sections of hearts from each group. Brick red-stained area represents viable myocardium, whereas the unstained (white) area represents infarcted myocardium. The ratio of IS/AAR **(C)** and AAR/LV **(D)** are shown. Representative echocardiograms **(E)** and measurements of different groups **(F)** were uniformly obtained from the mid-papillary muscle region of the left ventricle (LV). Ejection fraction (EF) **(G)** and LVFS **(H)** were measured by M-mode echocardiography (n = 5 of each group). Data were expressed as means ± SEM. * $P < 0.01$ vs. sham group, $^{\#}$ $P < 0.05$ vs. I/R group, § $P < 0.05$ vs. PD group, $^{\&}$ $P < 0.05$ vs. I/R + PD + 3-MA group. I/R, ischemia/reperfusion; NS, normal saline; PD, polydatin; 3-MA, 3-methyladenine; AAR, area at risk; IS, infarct size; LVFS, left ventricular fractional shortening.

Figure 4 Effects of PD on autophagic flux in cultured NRCs

(A) NRCs transfected with adenovirus harboring tandem fluorescent mRFP-GFP-LC3 (Ad-LC3-NRCs) for 24 h were subjected to different treatments. Representative pictures of immunofluorescent NRCs expressing mRFP-GFP-LC3. The nuclei were labeled with DAPI (blue staining), GFP dots are green, and mRFP dots are red. **(B)** Semi-quantitative analysis of autophagosomes (AP; yellow dots in merged images, white bars) and autolysosomes (AL; red only dots in merged images, black bars). **(C)** Western blot of LC3 in different groups with or without Baf, and the semi-quantitative analysis of LC3 II/I ratio and LC3 II/GAPDH were shown. $^{\#}$ P <0.05 vs. H/R + PD group. **(D)** Representative pictures of TUNEL staining and the quantitation of TUNEL-stained cells. * $P < 0.05$ vs. control

group, # $P < 0.05$ vs. H/R group, § $P < 0.05$ vs. H/R + PD group, & $P < 0.05$ vs. I/R + PD + Baf group. Data are representative of three independent experiments. Results are expressed as mean ± SEM. C, control; H/R, hypoxia/reoxygenation; PD, polydatin; 3-MA, 3-methyladenine; Baf, Bafilomycin A1.

Figure 5 Effects of PD treatment on mitochondrial function in NRCs exposed to H/R

(A) TEM pictures showing autophagosomes surrounded by double membranes (black triangle) and damaged mitochondria (swollen or ruptured mitochondria, indicated as dM). **(B)** ΔΨm was stained with JC-1 and measured by confocal laser scanning microscopy. **(C)** ΔΨm was stained with Rho 123 and measured by flow cytometry. Experiments were repeate for three times. Scale bar = 10 μm. * $P < 0.05$ vs. control group, # $P < 0.05$ vs. H/R group, § $P < 0.05$ vs. H/R + PD group. & $P < 0.05$ vs. H/R + PD + Baf group. C, control; H/R, hypoxia/reoxygenation; PD, polydatin; Baf, Bafilomycin A1.

Figure 6 Effects of PD on production of cellular ROS

NRCs were subjected to H/R and treated with 10 μM PD or 100 nM Baf or both. Cellular nonspecific ROS was stained with DCFH-DA and analyzed using confocal laser scanning microscopy **(A)** and flow cytometry **(B)**. H_2O_2 treatment (150 μM for 2 h) was used as a positive control. And N-acetylcysteine (NAC) (10 mM), a ROS inhibitor, also was applied. H_2O_2 was determined with an Amplex red hydrogen peroxide assay (C) and superoxide anion production was determined by using the SOD-inhibitable cytochrome c reduction assay (D). Scale bar = 10 μm. * $P < 0.05$ vs. control group, # $P < 0.05$ vs. H/R group, § $P < 0.05$ vs. H/R + PD group. & $P < 0.05$ vs. H/R + PD + Baf group; C, control; H/R, hypoxia/reoxygenation; PD, polydatin; Baf, Bafilomycin A1.

Figure 7 Illustration of actions and mechanisms of PD on myocardial I/R injury

Myocardial I/R causes mitochondrial damage, then leads to the release of ROS and apoptotic activation. PD enhances autophagic flux to clear damaged mitochondria to reduce ROS and cell death, and consequently limits myocardial infarct size.

Summary statement

This paper provides evidence that PD post-treatment alleviates myocardial I/R injury by promoting autophagic flux to clear damaged mitochondria to reduce ROS and cell death.

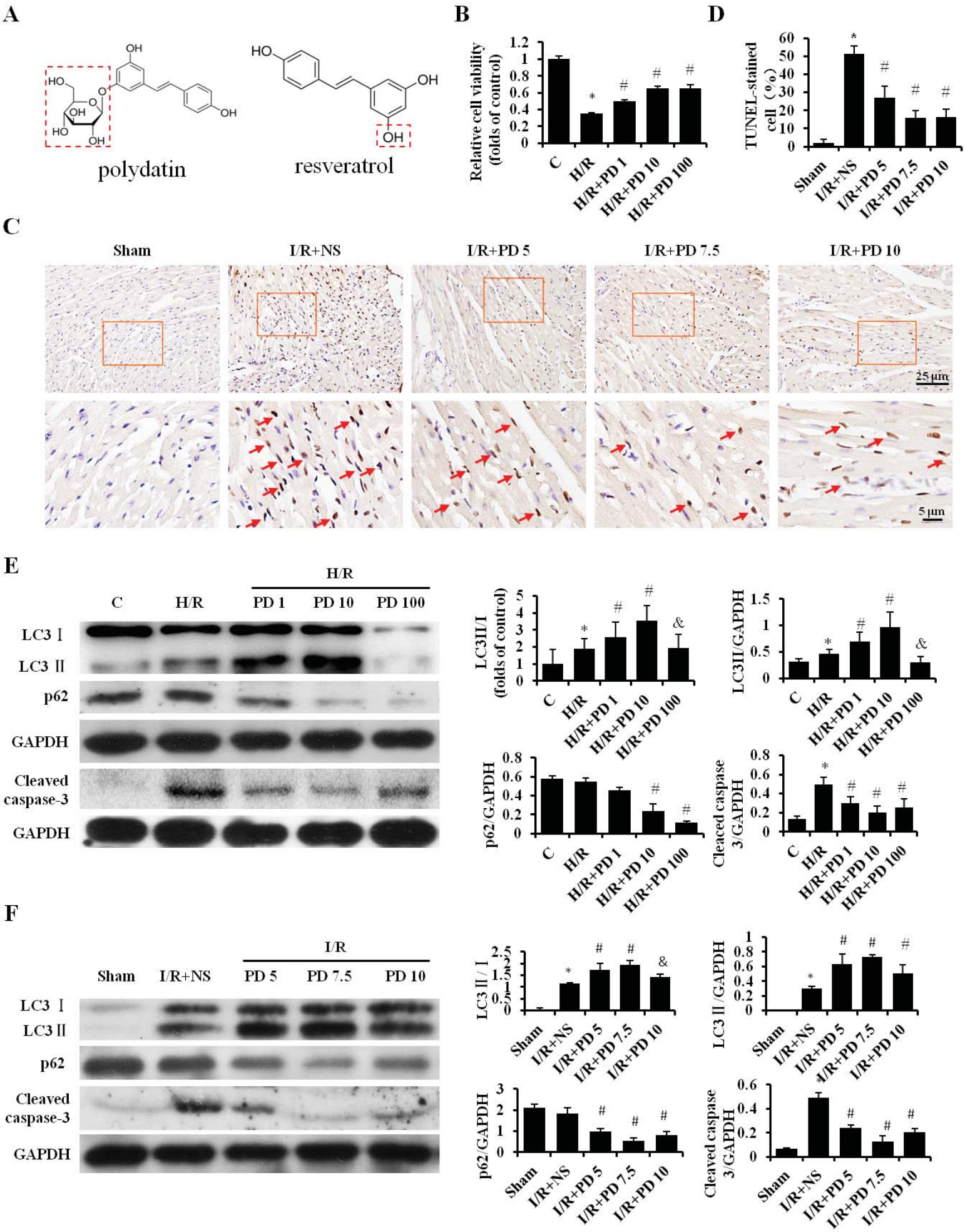
A
polydatin
resveratrol
B
Relative cell viability (folds of control)
C
H/R
H/R+PD 1
H/R+PD 10
H/R+PD 100
D
TUNEL-stained cell (%)
Sham
I/R+NS
I/R+PD 5
I/R+PD 7.5
I/R+PD 10
C
Sham
I/R+NS
I/R+PD 5
I/R+PD 7.5
I/R+PD 10
25 μm
5 μm
E
H/R
C
H/R
PD 1
PD 10
PD 100
LC3 Ⅰ
LC3 Ⅱ
p62
GAPDH
Cleaved caspase-3
GAPDH
LC3II/I (folds of control)
LC3II/GAPDH
p62/GAPDH
Cleaced caspase 3/GAPDH
F
I/R
Sham
I/R+NS
PD 5
PD 7.5
PD 10
LC3 Ⅰ
LC3 Ⅱ
p62
Cleaved caspase-3
GAPDH
LC3 Ⅱ/ Ⅰ
LC3 Ⅱ /GAPDH
p62/GAPDH
Cleaved caspase 3/GAPDH

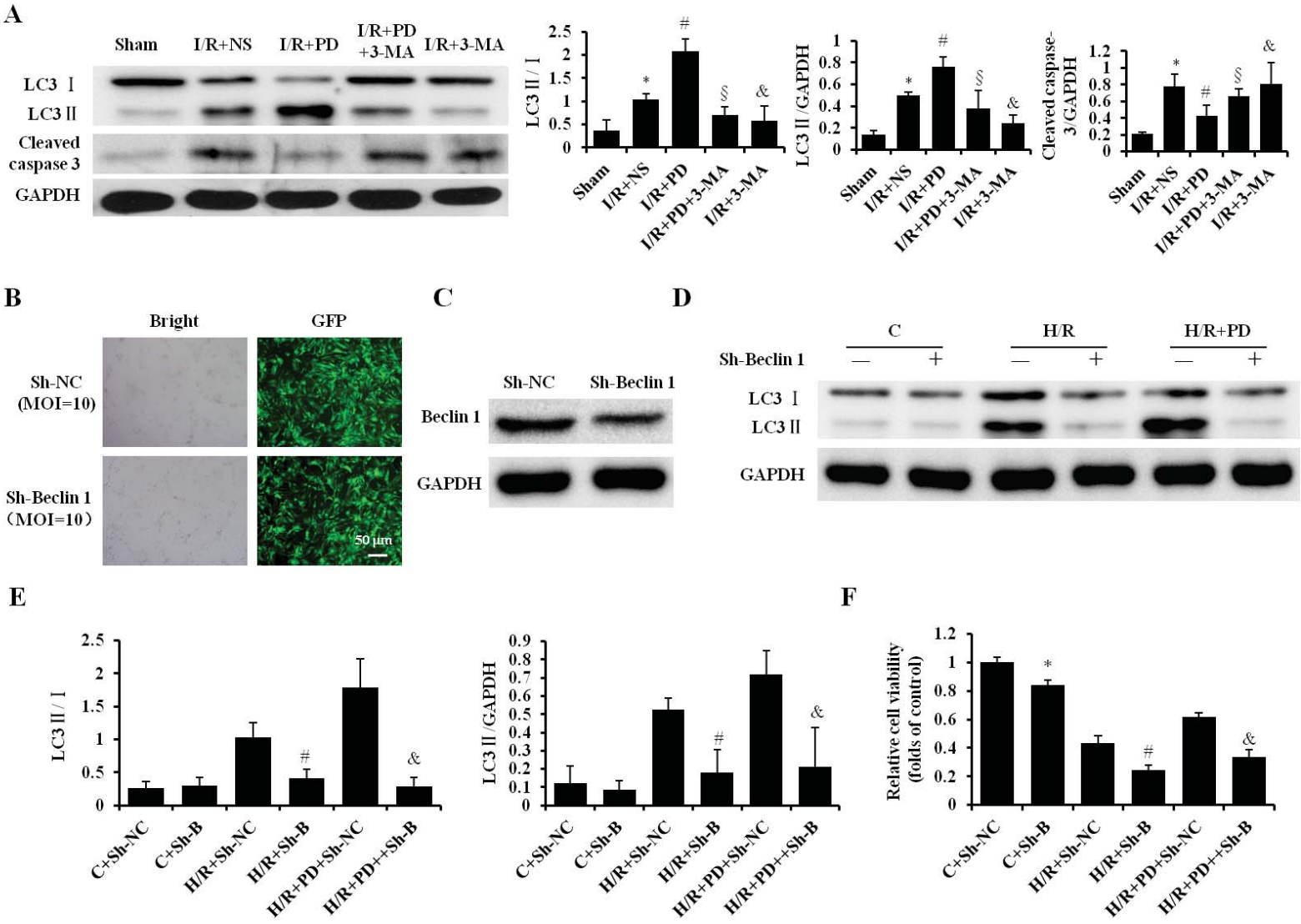
A
Sham
I/R+NS
I/R+PD
I/R+PD +3-MA
I/R+3-MA
LC3 Ⅰ
LC3 Ⅱ
Cleaved caspase 3
GAPDH
LC3 Ⅱ / Ⅰ
LC3 Ⅱ /GAPDH
Cleaved caspase-3/GAPDH
B
Bright
GFP
Sh-NC (MOI=10)
Sh-Beclin 1 (MOI=10)
50 μm
C
Sh-NC
Sh-Beclin 1
Beclin 1
GAPDH
D
C
H/R
H/R+PD
Sh-Beclin 1
LC3 Ⅰ
LC3 Ⅱ
GAPDH
E
LC3 Ⅱ / Ⅰ
LC3 Ⅱ /GAPDH
C+Sh-NC
C+Sh-B
H/R+Sh-NC
H/R+Sh-B
H/R+PD+Sh-NC
H/R+PD++Sh-B
F
Relative cell viability (folds of control)

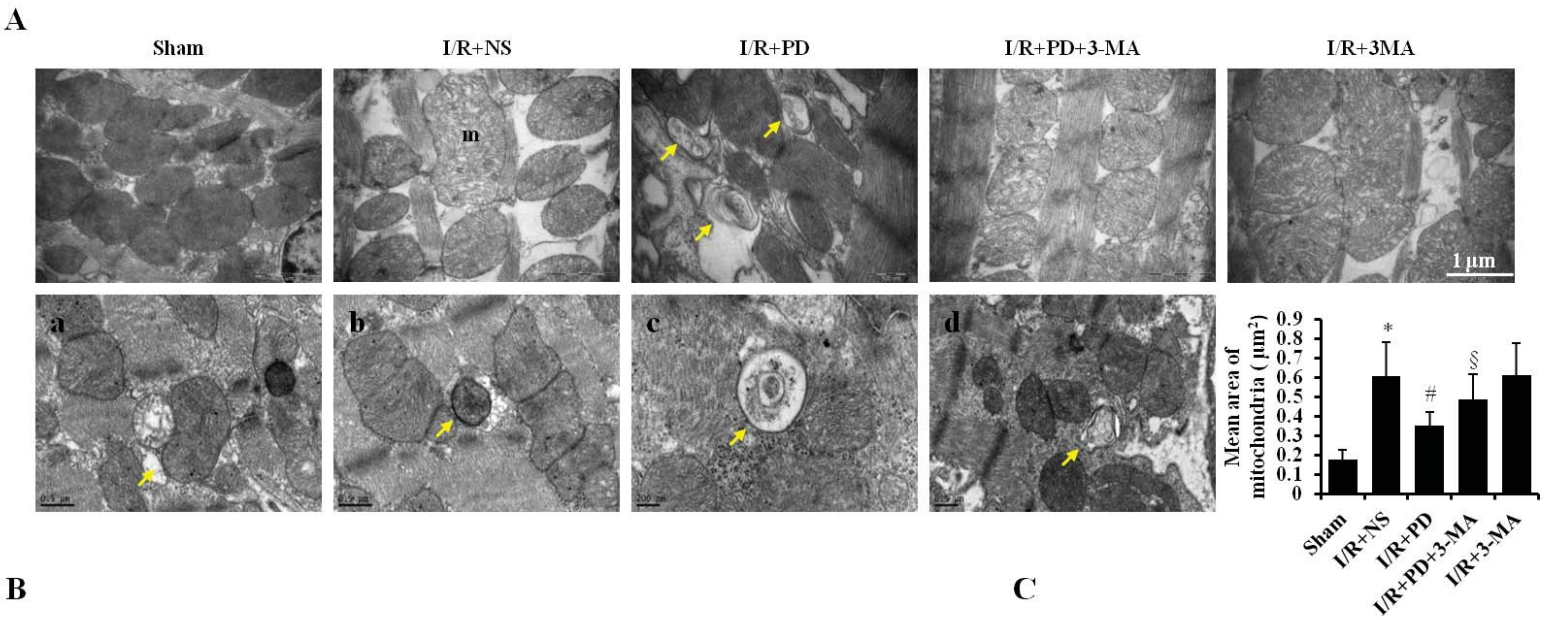
A
Sham
I/R+NS
I/R+PD
I/R+PD+3-MA
I/R+3MA
m
1 μm
a
b
c
d
Mean area of mitochondria (μm²)
0
0.1
0.2
0.3
0.4
0.5
0.6
0.7
0.8
0.9
*
#
§
Sham
I/R+NS
I/R+PD
I/R+PD+3-MA
I/R+3-MA

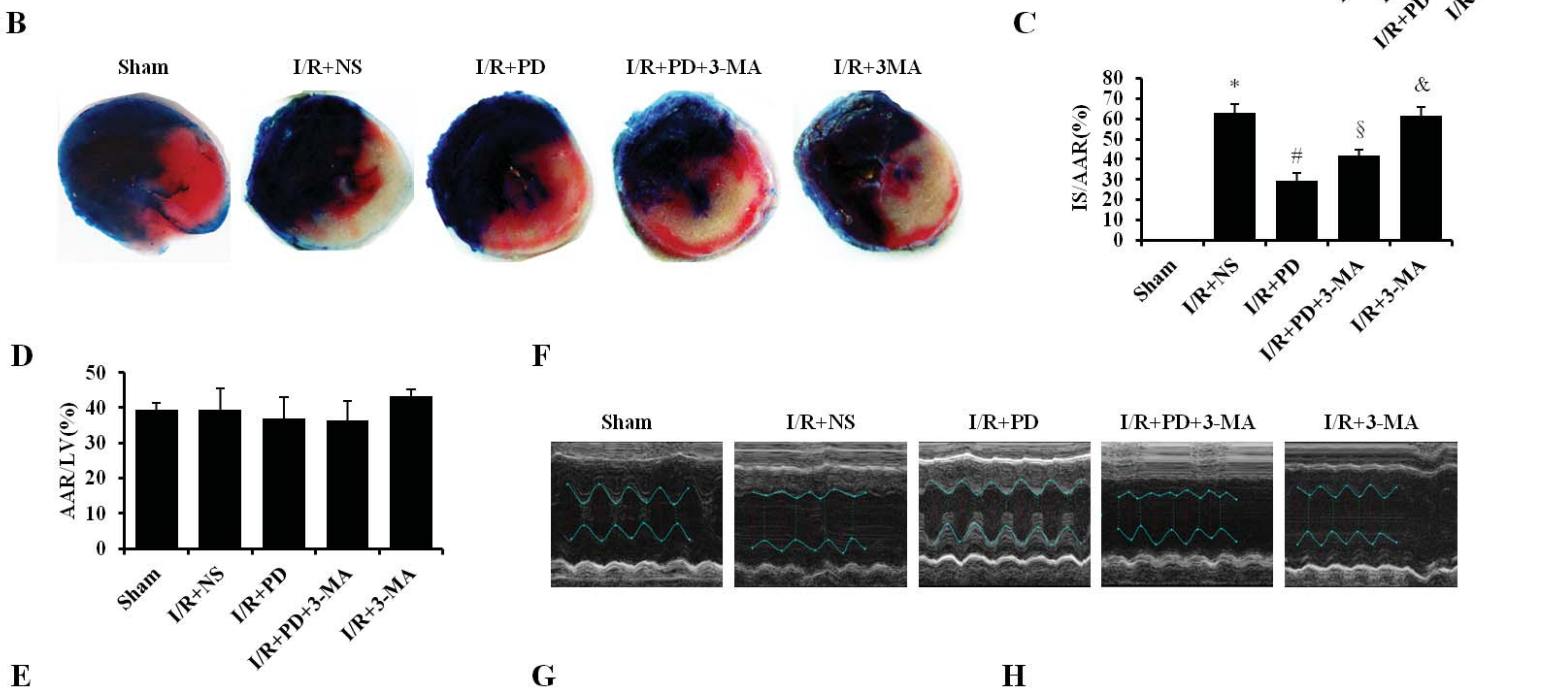
B
Sham
I/R+NS
I/R+PD
I/R+PD+3-MA
I/R+3MA
C
IS/AAR(%)
0
10
20
30
40
50
60
70
80
*
#
§
&
Sham
I/R+NS
I/R+PD
I/R+PD+3-MA
I/R+3-MA

D
AAR/LV(%)
0
10
20
30
40
50
Sham
I/R+NS
I/R+PD
I/R+PD+3-MA
I/R+3-MA
F
Sham
I/R+NS
I/R+PD
I/R+PD+3-MA
I/R+3-MA

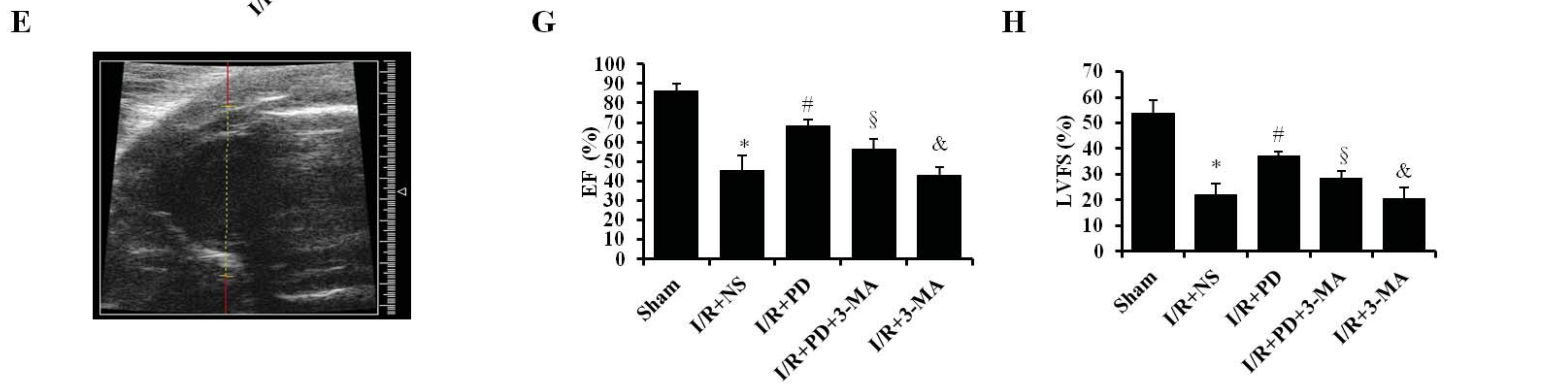
E
G
EF (%)
0
10
20
30
40
50
60
70
80
90
100
*
#
§
&
Sham
I/R+NS
I/R+PD
I/R+PD+3-MA
I/R+3-MA
H
LVFS (%)
0
10
20
30
40
50
60
70
*
#
§
&
Sham
I/R+NS
I/R+PD
I/R+PD+3-MA
I/R+3-MA

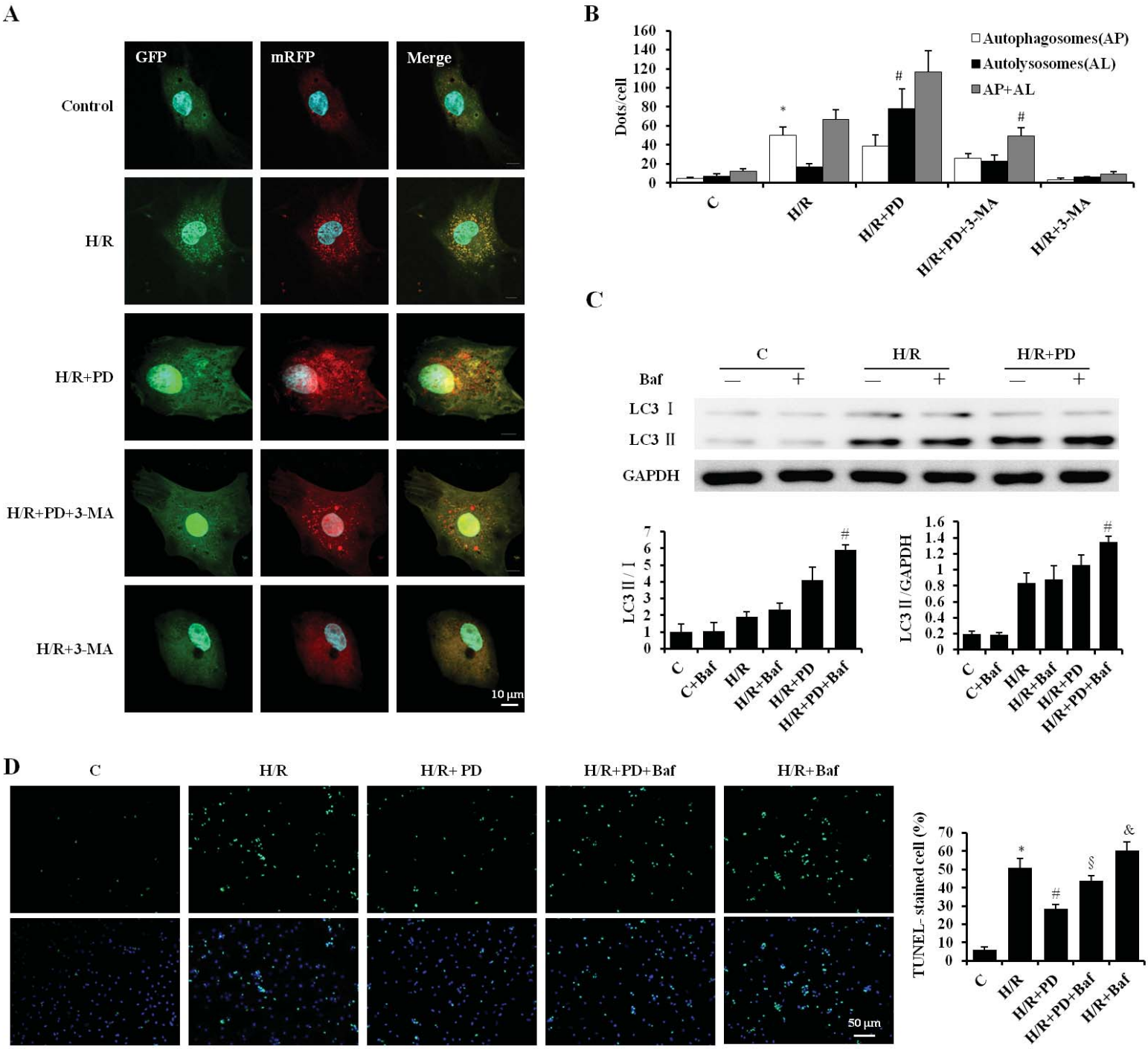
A
GFP
mRFP
Merge
Control
H/R
H/R+PD
H/R+PD+3-MA
H/R+3-MA
10 μm
B
Autophagosomes(AP)
Autolysosomes(AL)
AP+AL
Dots/cell
C
H/R
H/R+PD
H/R+PD+3-MA
H/R+3-MA
C
Baf
LC3 Ⅰ
LC3 Ⅱ
GAPDH
LC3 Ⅱ / Ⅰ
LC3 Ⅱ /GAPDH
C+Baf
H/R+Baf
H/R+PD+Baf
D
H/R+ PD
H/R+PD+Baf
H/R+Baf
50 μm
TUNEL- stained cell (%)

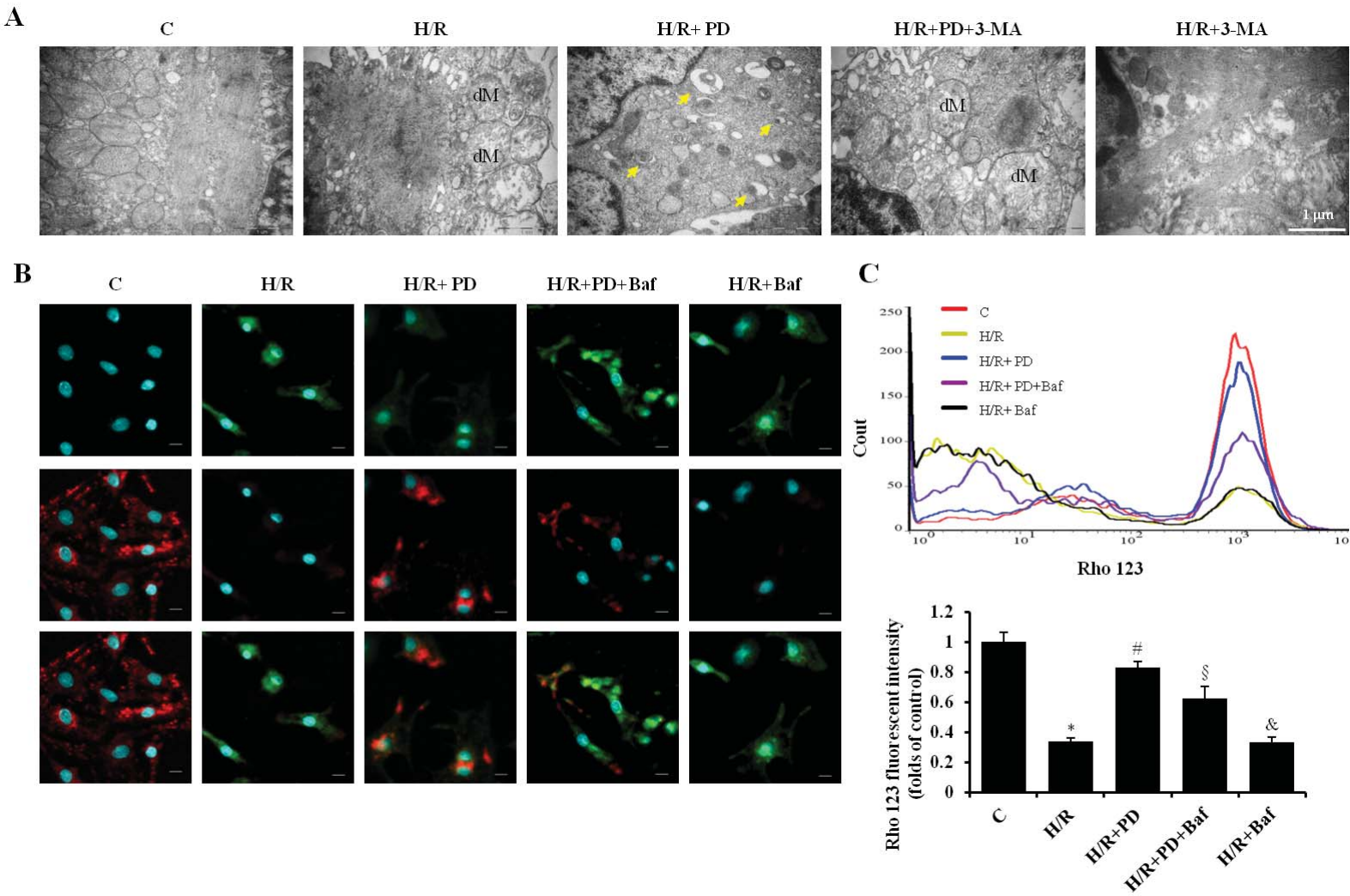
A
C
H/R
H/R+ PD
H/R+PD+3-MA
H/R+3-MA
dM
dM
dM
dM
1 μm
B
C
H/R
H/R+ PD
H/R+PD+Baf
H/R+Baf
C
250
200
150
100
50
0
Cout
C
H/R
H/R+ PD
H/R+ PD+Baf
H/R+ Baf
10^0
10^1
10^2
10^3
Rho 123
Rho 123 fluorescent intensity (folds of control)
1.2
1
0.8
0.6
0.4
0.2
0
*
#
§
&
C
H/R
H/R+PD
H/R+PD+Baf
H/R+Baf

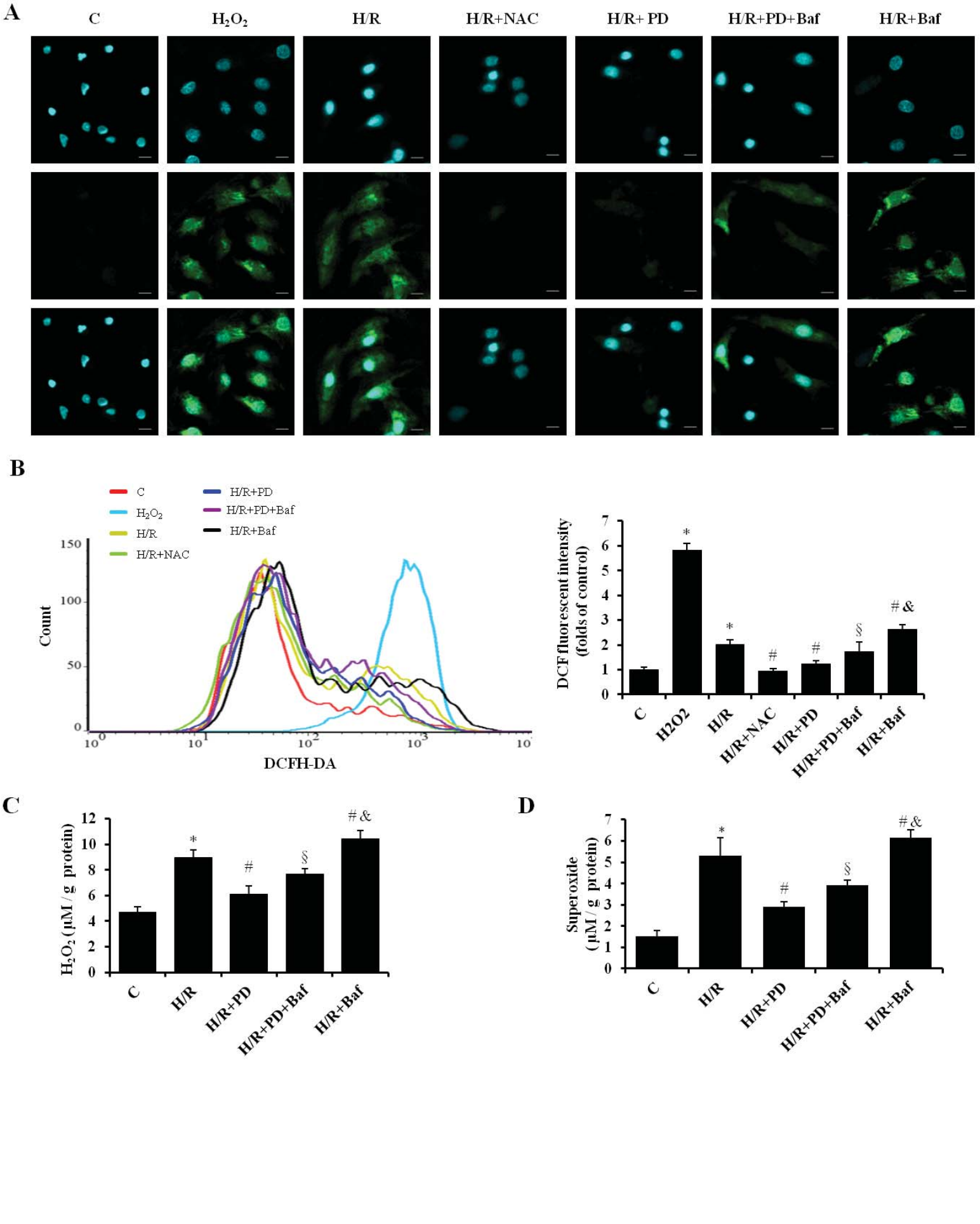
A
C
H2O2
H/R
H/R+NAC
H/R+ PD
H/R+PD+Baf
H/R+Baf
B
C
H2O2
H/R
H/R+NAC
H/R+PD
H/R+PD+Baf
H/R+Baf
Count
DCFH-DA
DCF fluorescent intensity (folds of control)
C
H2O2
H/R
H/R+NAC
H/R+PD
H/R+PD+Baf
H/R+Baf
C
H2O2 (μM / g protein)
C
H/R
H/R+PD
H/R+PD+Baf
H/R+Baf
D
Superoxide (μM / g protein)
C
H/R
H/R+PD
H/R+PD+Baf
H/R+Baf

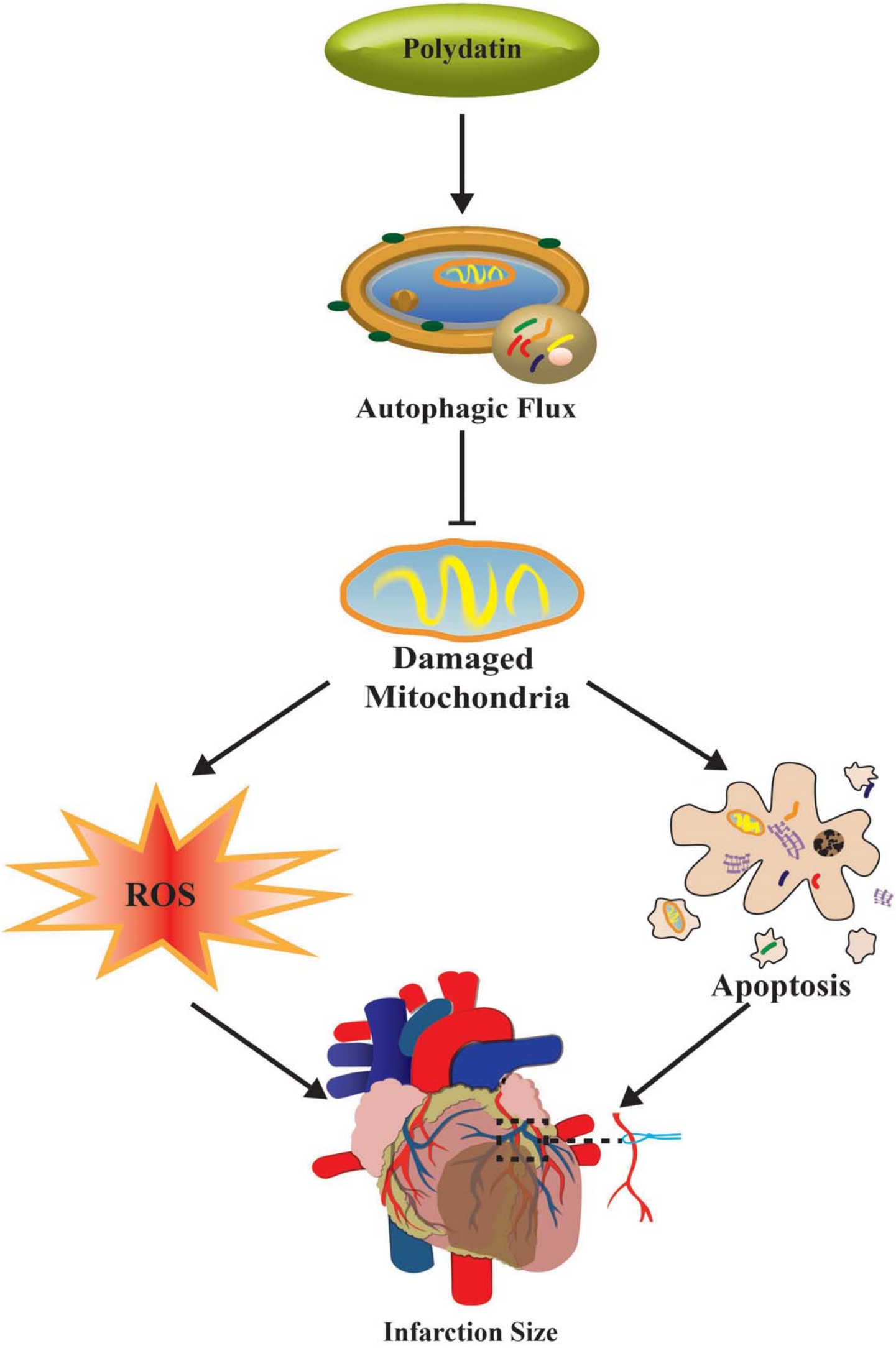
Polydatin
Autophagic Flux
Damaged
Mitochondria
ROS
Apoptosis
Infarction Size